HyMeX-SOP2, the field campaign dedicated to dense water formation in the north-western Mediterranean

Claude Estournel[1,a], Pierre Testor[2], Isabelle Taupier-Letage[3], Marie-Noelle Bouin[4, 8], Laurent Coppola[5], Pierre Durand[1], Pascal Conan[6], Anthony Bosse[2], Pierre-Etienne Brilouet[1,8], Laurent Beguery[7,b], Sophie Belamari[8], Karine Béranger[9], Jonathan Beuvier[10], Denis Bourras[11, c], Guylaine Canut[8], Alexis Doerenbecher[8], Xavier Durrieu de Madron[12], Fabrizio D'Ortenzio[5], Philippe Drobinski[9], Véronique Ducrocq[8], Nadia Fourrié[8], Hervé Giordani[8], Loic Houpert[13], Laurent Labatut[8], Cindy Lebeaupin Brossier[8], Mathieu Nuret[8], Louis Prieur[5], Odile Roussot[8], Leo Seyfried[1], Samuel Somot[8]

(1) Université de Toulouse; CNRS, Laboratoire d'Aérologie, Toulouse, France

(2) CNRS; IRD; UPMC Univ Paris 06; MNHN, LOCEAN, Paris, France

(3) Aix Marseille Université; CNRS; Université de Toulon ; IRD, MIO, 13288, Marseille, France

(4) CNRM/CMM, Météo-France – Brest, France

(5) Sorbonne Universités; UPMC Univ Paris 06 ; CNRS, LOV, Villefranche sur Mer, France

(6) Sorbonne Universités; UPMC Univ Paris 06 ; CNRS, LOMIC, Banyuls sur Mer, France

(7) INSU Division Technique, UPS 855, La Seyne sur Mer, France

(8) CNRM, UMR3589, Météo-France & CNRS, Toulouse, France

(9) CNRS; ENS; Ecole Polytechnique; UPMC, LMD, Palaiseau, France

(10) MERCATOR-OCEAN, Ramonville St Agne, France

(11) Université Versailles St-Quentin; Sorbonne Universités, UPMC Univ. Paris 06; CNRS, LATMOS-IPSL, Guyancourt, France

(12) Université de Perpignan; CNRS, Perpignan, France

(13) SAMS, Scottish Marine Institute, Oban, Argyll, United Kingdom

(a) : e-mail address: claude.estournel@aero.obs-mip.frmailto:claude.estournel@aero.obs-mip.fr

b : current address: ACSA, Meyreuil, France

c: current address: Aix Marseille Université; CNRS; Université de Toulon ; IRD, MIO, 13288, Marseille, France

Abstract

The HyMeX Special Observing Period 2 (SOP2, 27 Jan. -15 Mar. 2013) was dedicated to studying the dense water formation (DWF) in the gulf of Lion (north-western Mediterranean). The general set-up of the SOP2 and outlines of the meteorological conditions and of the oceanic deep convection for the winter 2012-2013 are described. Alternating mixing and restratification phases are related to periods of respectively high and low heat losses. High-resolution realistic 3D models appear to be essential to assess the intricacy of buoyancy fluxes, horizontal advection and convective processes. At submesoscale, vertical velocities resulting from symmetric instabilities of the density front bounding the convection zone are crucial for the ventilation of the deep ocean. Finally, concomitant atmospheric and oceanic data extracted from the comprehensive SOP2 data set highlight the rapid coupled evolution of the oceanic and atmospheric boundary layers characteristics during a strong wind event.

1. Introduction

Observations of oceanic convection leading to dense water formation (DWF) have been reported in a variety of regions: Greenland, Labrador, Mediterranean and Weddell Seas (see Marshall and Schott

(1999) for a review). DWF encompasses three phases (MEDOC group, 1970): (1) the preconditioning due to the basin-scale doming of isopycnals, (2) the convective phase, with the development of convective plumes (characterized by high down- and upward vertical velocities) and the formation of the mixed patch with associated eddy activity within it and on its edge, (3) the spreading phase, in which baroclinic instability is a key mechanism orchestrating the exchange of fluid and buoyancy with the surrounding stratified waters. Although these phases have been described separately, questions remain about their overlapping probably related under realist conditions, to intermittencies in the convection driver *i.e.* atmospheric forcing (Houpert et al., 2016). Temporal scales of the dynamical processes in the atmosphere and in the ocean are indeed close to each other during periods of oceanic convection: strong wind events with high heat and freshwater exchanges between the ocean and the atmosphere have a typical duration of a few days. The water column can mix over a temporal scale of the same order. Concerning the spatial scales, there is no significant separation between the convective and the baroclinic eddy scale (Marshall and Schott, 1999). These authors emphasize the "fascinating and central aspect of the convective process in the ocean, which is the interaction between convection and baroclinic instability". If buoyancy is extracted rapidly through violent events, baroclinic instability does not have enough time to limit the convection depth whereas, in the case of lower cooling rates, baroclinic instability may indeed control the depth reached by the mixed layer (Visbeck et al., 1996). This is probably a major reason explaining that no relationship has been proved between the volume of water formed, its hydrological characteristics and the atmospheric forcing (for example the heat and water losses integrated over winter).

The study of the interaction between horizontal and vertical processes under realist conditions is itself complex because (1) the need of a data set able to describe the variability of convection at small spatial scale (a few kilometers) and at high frequency (typically the day), (2) the difficulty of making accurate concomitant observations throughout the water column and the atmosphere during wintertime, (3) the uncertainties (especially for strong wind events) on the bulk formulae used to calculate air/sea fluxes and the frequent underestimation of very strong winds by atmospheric models (Hauser et al., 2003). The latter point is also a major sticking point for oceanic models. Moreover, it is

known that the eddy-permitting models used for climate studies overestimate DWF compared to eddy-resolving ones (Herrmann et al., 2008) as the exchanges between the mixed patch and the stratified waters are reduced by the lack of mesoscale eddies. A question thus remains about the need of parameterizations to avoid drifts of climatic simulations.

Then, the objectives of the HyMeX-SOP2 were to study how the different oceanic processes interact during convection, how this interaction is related to atmospheric fluxes and how numerical models with different spatial resolutions (typically from 1 to 10 kilometres) are able to simulate convection. The choice of an appropriate strategy, including the experimental site, was a major issue for the achievement of these objectives. The Hydrological cycle in the Mediterranean Experiment (HyMeX, 2010-2020; Drobinski et al., 2014) fosters the synergy of communities aiming, *inter alia*, at monitoring and modelling the Mediterranean atmosphere-land-ocean coupled system, its variability and its long-term evolution. A first Special Observing Period (HyMeX-SOP1, 15 Sept. - 15 Nov. 2012) was dedicated to the high-precipitating events and flash-floods (Ducrocq et al., 2014). The HyMeX-SOP2 (27 Jan. -15 Mar. 2013) was dedicated to studying the dense water formation in the Gulf of Lion (north-western Mediterranean). The goal was to acquire a data set sufficiently extensive in space and time, first of all, to study the processes governing the dense water formation and spreading and their interactions at the scale of the meteorological events, and then, to test the ability of ocean models at different horizontal resolutions to reproduce the characteristics of the newly formed dense water. The Mediterranean basin is particularly suitable for deep water formation studies, for at least three reasons: i) long-term monitoring already exists and provides a longer time frame perspective to this short-term experiment, ii) the spatial scales involved are smaller there than in the open oceans, iii) the atmospheric and sea state conditions are somewhat milder than in polar regions facilitating the deployment of instruments at sea.

Convection in the Gulf of Lion is allowed by the prevailing cold, dry, northerly local winds (Mistral and Tramontane) inducing high cooling and evaporation, and by the cyclonic circulation associated to the doming of isopycnals, which facilitates mixing with the saltier underlying waters. During winter,

the cyclonic circulation is reinforced isolating water in its central part, which favours heat losses. Convection in the Gulf of Lion shows an important interannual variability, both in time (years with or without DWF) and in space: the vertical extent of the convection varies between a few hundred of meters and the whole water column (~2500 m) (Mertens and Schott, 1998; Somot et al., 2016), and its horizontal extent from a few tens of kilometres to ~ 100 km in radius. This convection feeds a thermohaline circulation through the transformation of water of Atlantic origin into intermediate and deep water masses, the Winter Intermediate Water (WIW) and the Western Mediterranean Deep Water (WMDW). During the spreading phase, about 50% of the newly-formed dense water would be incorporated in the Northern Current, the other part being transported far away by numerous and long-lived eddies (both anticyclonic and cyclonic) (Send et al., 1996; Testor and Gascard, 2006; Bosse et al., 2016).

This paper first describes the HyMeX-SOP2 general set-up designed to grasp the wide span of temporal and spatial scales of the processes involved in DWF. Then the meteorological and convection characteristics of the winter 2012-2013 are presented. The succession of mixed and stratified vertical profiles of density is put in relation with the intermittencies of atmospheric forcing. The role of the vertical and horizontal processes including the submesoscale ones, in the convection is then discussed. Finally a data set collected in both the atmosphere and ocean during a late convection event is presented. The description of the huge data sets collection is also intended to raise the interest of scientists to join a similar experiment in the eastern basin of the Mediterranean expected in a few years.

2. Experimental design at various temporal scales

The monitoring of the north-western Mediterranean, following the HyMeX observation strategy, was organized at three different temporal scales, from the interannual one to the seasonal one addressed by the SOP2. The interannual scale (Long Observation Period) is achieved by the MOOSE (Mediterranean Ocean Observing System for the Environment - http://www.moose-network.fr/)

integrated observing system aiming at observing the impact of climate on the evolution of the hydrology and biogeochemistry of the north-western Mediterranean. On the annual scale named Enhanced Observation Period, monitoring the water column stratification was also a priority: a first reason was the need for initial conditions in summer, to assess a budget of dense water (difference of volume and changes in density before and after winter). The second reason was the central role of autumn in the seasonal cycle, corresponding to the preconditioning phase and the first deepening of the mixed layer. The Enhanced Observation Period benefited from the synergy of several programmes: MOOSE, MERMEX (Marine Ecosystems Response in the Mediterranean Experiment), and the HyMeX SOP1.

Finally on seasonal scale, SOP2 focused on the oceanic mixed layer deepening by convective processes, was based on the intensification of the existing monitoring network and on specific deployments targeting the most interesting events. Figure 1 presents the topography of the north-western Mediterranean with the positions of the instruments used at the different temporal scales and described below.

Long-term and Exhanced Observation Periods

Two Météo-France moored buoys, the LION buoy in the Gulf of Lion and the AZUR in the Ligurian Sea, measure the parameters needed for the calculation of the heat and water budgets through bulk formulae (namely atmospheric parameters, radiative fluxes, and sea surface temperature), and the wave spectra with an omnidirectional waverider. These two buoys are also equipped with 20 temperature sensors to document the first 250 meters of the water column and with a surface salinity sensor. These measurements complete the vertical profiles acquired between 150 and 2300 meters by the LION mooring supported by MOOSE and available since 2007. This mooring, less than 5 km from the LION surface buoy, includes 21 temperature and 15 salinity levels.

Thanks to MOOSE and the European PERSEUS programme, numerous glider deployments (13 in 2012) were performed in the Ligurian Sea and in the Gulf of Lion measuring depth-average currents,

temperature, salinity and dissolved oxygen as well as other biogeochemical variables like Chl-a fluorescence and turbidity

A ship of opportunity (Marfret-Niolon) making a weekly crossing between Marseille and Algeria provided information on the N-S, cross-basin variability of the air-sea characteristics by continuously recording the sea surface temperature (SST) and salinity (SSS) and the meteorological parameters.

At regional scale, MOOSE carries out every summer a survey of the stratification of the water masses. In August 2012 and June 2013, 80-90 conductivity-temperature-depth (CTD) casts were performed. In September 2012, February 2013, April 2013 and September 2013, similar cruises were organized by the MERMEX programme on the same network (Waldman et al., 2016). The August 2012 cruise used to improve the initial stratification of the models has proved to be crucial to represent DWF (Estournel et al., 2016).

Special observation period

HyMeX SOP2 documented the DWF zones of the north-western Mediterranean, i.e. mainly the Gulf of Lion and, to a lesser extent, the Ligurian Sea, where dense waters are formed more exceptionally. In situ measurements during strong wind events are always challenging (winds above 25 m/s and waves as high as 7 m (H1/3) were recorded at the LION buoy). Thus the strategy was designed both to allow near-real-time response, and to foster autonomous platforms less affected by the weather and sea conditions.

a. Observations at the air-sea interface and in the upper water column

Several surface drifters were deployed: five Marisonde buoys measuring near-surface atmospheric pressure, wind, and air temperature and equipped with a 300-m-long thermistor chain, and seven SVP drifters, some of them equipped with an 80-m-long thermistor chain, and the others equipped with SST and SSS sensors.

As ship time on the French oceanographic fleet was granted for scientific cruises at fixed periods (RV "Tethys II", RV "Le Suroit"), the seagoing buoy tender vessel "Provence" was chartered to complete the need for in situ observations. Direct measurements of air-sea turbulent and radiative fluxes onboard (Bourras et al., 2009) were performed using a set of instruments installed on the top of a bow mast. Three different methods were used to calculate the turbulent fluxes: the bulk method, the inertial-dissipation method, and the eddy-covariance method.

b. Deep ocean observations

During winter 2012/13, the evolution of thermohaline characteristics of the water masses was also monitored at high frequency through the deployment of a large number of autonomous profiling floats and gliders as well as through dedicated ship cruises. Four Argo floats equipped with oxygen sensors were added to the 6 existing floats in the Gulf of Lion. They were dedicated to documenting the mixing in the deeper oceanic layers. Consequently, the type of floats used during this observation period were enabled with the capability of switching from the classical MedArgo cycle of 1 profile over 1000 m every 5 days, with a parking depth at 350 m, to a "DWF" cycle of 1 full-depth profile (2000 m) daily with a parking depth at 1000 m. This strategy aimed at monitoring the water column thermohaline changes at high frequency and at minimizing the floats drift to increase their presence in the convective zone.

During SOP2 period, up to 9 gliders were deployed at the same time from the Balearic Islands to the Ligurian Sea. They documented the upper 1000 metres at high spatial resolution (profiles spaced about 4 km apart) and at high frequency (of the order of 6 dives per day).

About 100 CTD casts were made during the 20-day DEWEX cruise aboard the R/V Le Suroît organized by MERMEX (3-21 February 2013) and during the few-day cruises of the R/V Tethys II (29-30 January and 20-21 February 2013) and the buoy tender vessel "Provence" (7-10 March 2013).

c. Observations in and above the marine atmospheric boundary layer

Marine and atmospheric boundary layers interact through surface fluxes of heat, moisture and momentum. These fluxes are dependent on the air temperature, moisture and wind and, in turn, modify these parameters. The atmospheric boundary layer (ABL) is generally well mixed but presents noteworthy discontinuities at the interface with the upper free troposphere. The fluxes at the top of the ABL are able to modify by entrainment the "bulk" characteristics of the ABL and hence the surface fluxes. For this reason, it was decided to document not only the surface fluxes, but also the turbulence structure of the whole ABL, up to the upper interface with the free troposphere.

The French ATR42 aircraft documented the air mass during strong wind conditions. The aircraft was equipped to measure turbulence fluctuations, thus allowing turbulent fluxes to be computed through the eddy correlation method, as well as turbulence parameters (Canut et al., 2010). Usually, 6 to 8 legs were made during the flights, from 150 m to about 1200 m. The level of the different legs was adjusted, based on the ABL thickness obtained from an initial vertical profile.

Fifteen boundary layer pressurized balloons were launched near Montpellier airport (M1 in Fig.1) to drift at constant density levels over the sea and to sample temperature and humidity along the path of the air mass (Doerenbecher et al., 2016). In addition, thirty-eight radiosoundings were launched, some of them at Montpellier to better choose the flight level of the balloons and the others at Marseille (M2 in Fig.1) and onboard the "Provence". Finally, a network of five coastal UHF radars, four of them around the Gulf of Lion and one in Corsica, measured the vertical profiles of wind from 100 m to 4 km every 15 minutes.

d. Science and operations coordination

The SOP2 field campaign lasted from 1 February to 15 March 2013. During this period, several episodes of strong, cold winds occurred, resulting in the progression of oceanic convection down to the seafloor.

As described for HyMeX-SOP1 (Ducrocq et al., 2014), scientific staff decided on science missions, intensive observation periods and the deployment of on-demand instrumented platforms. Decisions were based on an analysis of the outputs of atmospheric and ocean forecast models and of the recent oceanic observations mostly available in near-real time.

The SOP2 experiment was undoubtedly the one that provided the largest number of T and S profiles during a DWF period in all oceanic convection areas. About 100 CTD profiles are available from the surface to the bottom and 250 Argo profiles between 0 and 2000m. The number of glider-days between January and March was about 350, providing about 2000 profiles between 0 and 1000 m.

3. Meteorological characteristics of winter 2012-2013

The winter wind regime in the Gulf of Lion is usually characterized by alternating situations of strong northerly or north-westerly wind (Mistral and Tramontane) and moderate easterly to southerly wind associated with precipitation. Mistral and Tramontane are orographic winds bringing continental dry and cold air over the Gulf of Lion, and inducing intense heat, freshwater and momentum exchanges with the sea surface. In the following, we refer largely to the atmospheric and subsurface parameters observed at the LION buoy, representative of the atmospheric conditions above the Gulf of Lion DWF area. Figure 2 presents the wind speed and direction, the difference between sea surface and air temperatures and the difference between the saturated specific humidity over seawater and the air specific humidity measured at the LION buoy. These quantities determine the sensible and latent heat fluxes (and thus the evaporation). A statistical analysis was performed to compare the measurements for the SOP2 period to a 10-year climatology made with the buoy measurements from December to

February between 2002 and 2011. SOP2 values were very close to the climatology for the mean wind but also for the strongest winds (95th and 99th percentiles of the climatology – Q95 and Q99 in the following – were equal to 17.8 and 20.2 m/s respectively). The extreme values of temperature and specific humidity differences were clearly more frequent during winter 2012-2013 than in the climatology (temperature difference: Q95=6.5°C, Q99=7.7°C; specific humidity difference: Q95=5.4g/kg, Q99=6.7g/kg). Temperature difference exceeded Q95 during 12.2 % of the period and specific humidity difference during 10.9%. The corresponding wind direction (Figure 2) was northerly to northwesterly, bringing cold and dry air (maximum temperature difference 9.8°C, maximum specific humidity difference 5.9g/kg). This indicates that winter 2012-2013 experienced stronger-than-average air-sea exchanges (rather due to the air-sea temperature and humidity gradient than to the wind speed).

The corresponding radiative and turbulent fluxes (Figure 3a) clearly show that the major heat and water losses are due to the latent heat flux. While the solar radiation daily maximum still reaches values higher than 400 W/m^2 during Mistral/Tramontane events, the turbulent heat fluxes (latent, and to a lesser extent sensible flux) can more than compensate this heat transfer on several consecutive days, as shown by the resulting net heat flux (Figure 3b). In order to evaluate the uncertainty brought into the turbulent fluxes estimates by the bulk formulation used, net heat fluxes resulting from several widely-used bulk formulae are compared in Figure 3b. The COARE 3.0 algorithm (Fairall et al., 2003) has been used with different formulations of the surface roughness: (i) with a constant Charnock parameter (COARE), (ii) using the Oost et al., (2002) formula relating the surface roughness to the wave age only (COARE 1), and (iii) with the Taylor and Yelland (2001) formula using the peak period and the significant wave height (COARE 2). The results of the algorithms of Andreas et al., (2008) accounting for sea spray, Moon et al., (2007) and Ecume (Belamari and Pirani, 2007) which is used in the Météo-France models are also presented. Observed wave parameters and atmospheric and ocean surface parameters at the Lion buoy have been used to process the corresponding turbulent fluxes. The mean heat loss as seen by all the algorithms is of -126 +/- 11 W/m^2 on the SOP2 period and, if we restrict to the wind speeds above 15 m/s (as most prone to trigger DWF), of 548 +/- 26 W/m^2. The

maximum difference on hourly values of the net heat flux obtained by using different algorithms is 239 W/m^2). Turbulent heat fluxes are also estimated from the lowest legs of aircraft, approximately at 150 m above the sea. They corroborate tendencies based on bulk formulae even if differences are observed. A method of correction of airborne data is currently developed for extrapolating down to the surface the heat fluxes deduced from airborne measurements which are one of the only direct sources of information.

4. Characteristics of convection during winter 2012-2013

Being based on a threshold of the vertical density or temperature gradient, the calculation of the mixed layer depth (MLD) in the Mediterranean is faced with the problem of low gradients under the surface layer (0 to ~ 300 m) making difficult the tracking of convection with this index. On the opposite, the stratification index is an objective measure of the amount of buoyancy which should be extracted to achieve the complete mixing of the water column. This stratification index has been calculated (Eq. 1) for all the available T,S profiles measured with the CTD and the Argo floats. It was then mapped on Fig. 4a and a composite time series is proposed in Fig. 4b.

$$SI(Z) = \int_{-Z}^{0} \big(\rho(Z) - \rho(z)\big)\, dz \qquad (1)$$

where ρ is the potential density, SI is expressed in kg m^{-2}. Our reference level Z is 1500 m. When $SI = 0$ it means that the water column is mixed at least over the 1500 m upper layer ($MLD > 1500m$).

During January 2013, the stratification regularly decreased. Vertical mixing reached 1500 m (black dots) at the beginning of February. Such a deep mixed layer is continuously observed at one point or another until the first days of March. Then, a restratification equivalent to 5 kg m^{-2} appears during a period of low heat losses (Fig. 3). On 14 March, SI abruptly falls again to very low values with an intense event of strong wind associated to strong heat losses (Figs 2 and 3). Deep mixing is classically centered in the Gulf of Lion around 42°N, 5°E while mixing is on average shallower in the Ligurian

Sea. Highly stratified waters encircle the convection zone (red and gray dots) along the general circulation sketched in Fig.1.

5. Convection: vertical and horizontal processes

To compare the impact of surface fluxes and horizontal advection on the convective processes, we carried out 1D vertical simulations (without horizontal advection) at the LION mooring location with the SYMPHONIE model (Marsaleix et al., 2012). These simulations were initialized on 6 December 2012, with mooring measurements for deep water and a glider (which was close to mooring at this date) for intermediate and surface water. They were forced at the surface by buoyancy surface fluxes calculated with 3-hourly ECMWF operational forecasts extracted at the LION mooring position. To take into account the uncertainties on the turbulent heat fluxes, we used two bulk parameterizations, COARE and MOON (see section 3), which provide respectively the lowest and the strongest fluxes (Fig. 5a).

The temperature profiles calculated with these simulations, named respectively COARE and MOON, were compared in Fig. 5 with the LION mooring measurements. Simulations start with a stratified profile, then successive strong wind events with strong buoyancy losses mixing the water column are observed and simulated. However, the oceanic convection begins earlier in the simulations due to a too strong heat loss, particularly in MOON. Convection simulated with MOON reaches 1500 m in January, that is 20 days before it was detected by the observations. Moreover, in February, both simulations present unrealistic low temperature. These simulations suggest that the horizontal advection by baroclinic instability omitted in this 1D vertical approach is a major factor controlling the MLD. Indeed, during the periods of positive buoyancy surface flux, the observations show restratification events in the first 500 meters (see patches of warming), which limit the progress of convection and subsequent cooling once the complete mixing of the water column is reached. Studies with high-resolution realistic 3D models are essential to understand the complex interactions between buoyancy fluxes, horizontal advection and convective processes (see Estournel et al., 2016 for a heat

and water budget over the preconditioning and convective periods). Another conclusion is that the uncertainties on turbulent heat fluxes have to be reduced.

6. Submesoscale processes

Autonomous underwater gliders are oceanic observing platforms well suited to capture the small scale variability in convective regions. Submesoscale flows are greatly enhanced during winter as lateral density gradients becomes more intense (Callies et al., 2015), being then responsible for intense vertical exchanges. Those processes are though still poorly understood, and this mostly due to a lack of in situ observations.

Figure 6 indicates the trajectory of a glider crossing the deep convection area in February 2013. The along-track temperature and isopycnals from the surface to 1000 m depth (figure 6 lower right panel) clearly show the mean cyclonic circulation circling the convection zone in the central part of the Gulf of Lion. By that time, the Northern Current and North Balearic Front were both characterized by a strong density gradient separating the surface Atlantic Water (AW) and underlying warm Levantine Intermediate Water (LIW) from the newly-formed deep water. The lateral buoyancy gradients ($b = -g\,\rho/\rho_0$ being the buoyancy, ρ the potential density and ρ_0 a reference density) between the convection zone and the rim current were very intense, reaching 1-2 10^{-7} s^{-2} (see figure 6 upper right panel). On the other hand, the vertical stratification ($N^2 = db/dz$) characterizing the static stability of the water column is drawn to almost zero in the central part of the Gulf of Lion as a result of the vertical mixing. Regarding the stability of those density fronts, the potential vorticity is a key parameter that can be approximated as the difference between a vertical stratification term $A = N^2 f^2$ (where f is the Coriolis parameter) and the square of the along-track buoyancy gradients $B = (db/dx)^2$ (Thomas et al., 2013). A negative potential vorticity is the condition for symmetric instability. For the sake of clarity, as well as to avoid numerous technical details, we have neglected here the vorticity of the currents much smaller than f for geostrophic flows. The glider sampled the Northern Current front twice within 4 days (between points B and A) revealing its rapid evolution. On

February 15 (figure 6b lower panel left), the temperature exhibited interleaving of warm and cold waters at submesoscale suggesting the presence of important vertical exchanges while four days later, the front was restored back to a stable situation. Moreover, the negative potential vorticity revealed that the front area was symmetrically unstable during the first crossing. Winter fronts around the deep convection zone can thus be unstable to symmetric instability, which is known to result in triggering slanted motions connecting the surface waters to the deeper levels below the stratified front. Our observations suggest that this process recently observed in the Gulf Stream (Thomas et al., 2013), could also play a crucial role in the ventilation of high- and mid-latitude deep convection zones. Of course, this process acts in concert with other sources of vertical velocities in the ocean like static instability or frontogenesis (Giordani et al., 2006). Finally, the section crossing the Balearic Front (around point C) also revealed the presence of cold waters down to about 600 m. This further reinforces the idea that vertical velocities are active at the edge of the deep convection area and are crucial for the ventilation of the deep ocean.

Finally, it is also noteworthy that, while exploring the western slope of the Gulf of Lion around the Lacaze-Duthiers canyon (Point B), the glider recorded a moderate cascading event of shelf waters (see indication of the location on the figure) characterized between 0 and 650 m by colder (12.5°C) and fresher (38.2) waters compared to the Gulf of Lion.

7. Complementarity of the data set: the example of an intense observation period (IOP28 - 13-15 March 2013)

A strong wind event occurred from March 13 to 15 after a week of calm weather (see section 4). Figure 7 shows the 10-m winds from the SOP-dedicated AROME weather prediction system at 2.5 km resolution (AROME-WMED, Fourrié et al., 2015) on March 14 at 12 UTC and the 10-m winds measured at the LION buoy (middle panel). They both show Mistral/Tramontane northwest winds reaching 30 m/s in the western Gulf of Lion. The aircraft flew close to the LION buoy on 14 and 15 March and recorded wind speeds of 20 m/s near the surface, and up to 30 m/s in the upper half of the

ABL near 1000 m (not shown). The cooling associated with the strong northwesterly winds led to a decrease of 7°C of the air temperature in 48 hours at the buoy. Air and sea surface temperatures, which were both close to 13°C before the event differed thus by 7°C on March 15. The air temperature drop recorded by the aircraft on March 14 and 15 was similar to that observed by the buoy during the same interval (see the "Aircraft" insert). Figure 7 ("Balloon" insert) also presents the specific humidity recorded by three pressurized balloons drifting between 600 and 900 meters above sea level on March 14 and 15. The regular increase of humidity along the path of the air mass over the sea reflects the evaporation at the air-sea interface which fills the ABL with water vapour which is then transported with the northwesterly winds. The quite similar values measured by the three balloons indicate a rather well mixed ABL. A large moisture difference was observed between the surface (buoy) and the ABL (see the "Aircraft insert" where the surface values have been reported), of the order of 3 g/kg, confirming large evaporation.

Such conditions were able to destroy the relatively strong oceanic stratification reigning in the first 200-300 m during the previous week (see the evolution of potential density recorded by Argo float 6901471– right panel- and the temperature recorded under the LION buoy). As discussed before, this stratification had been induced by horizontal advection during the phase of low wind of the beginning of March (Fig. 5a). The stratification is progressively erased from March 13. The surface potential density increased from 29.04 to 29.12 between March 12 and 15. A new ocean mixed layer of 200 m thickness is visible on the profile of March 14, and on March 15, the density profile became clearly unstable. Thanks to the quality and quantity of data collected in such situations, it will be possible to calculate budgets of heat and water in the atmospheric and marine compartments, to check the numerical models including coupled ocean-atmosphere-waves models and to address scientific questions linked to the consecutive phases of oceanic convection and the impact of intermittencies in the atmospheric forcing.

8. Conclusion

The north-western Mediterranean has been the subject during the HyMeX-SOP2 of a rather comprehensive description encompassing a large range of spatial scales from the regional scale to the submesoscale, and of temporal scales from the seasonal scale, with the three phases of dense water formation, to the hourly scale at the mooring sites. As a result, a large set of meteorological and oceanographic observations was collected.

The first results presented here indicate the importance of the exchanges between the mixed patch and its stratified periphery. The cooling of the water column in the mixed patch is disrupted by intrusions of warmer water. The observed cooling of the convection zone and thus the dense water production are then lower than predicted by a 1D modelling approach. Otherwise gliders reveal the presence of strong vertical velocities related to symmetric instability developing at the edge of the convection zone. These submesoscale processes contribute to the ventilation of the convection zone. Finally, the combination of atmospheric and oceanographic observations illustrate the fast response times of each medium, e.g., the destruction within hours of the ocean stratification or the temperature and humidity increase of the continental air mass over the sea.

Thanks to SOP2 observations, a fantastic benchmark is now available for modeling studies and for this particular year. Together with the ongoing and long term observational efforts carried out in the framework of MOOSE since 2010, we anticipate interannual variability issues could be soon addressed with fine tuned models.

Acknowledgements

Many people participated in SOP2: scientists, technicians, crews and people in charge of the organization. All deserve our grateful thanks. The HyMeX-SOP2 was supported by CNRS, Météo-France, IFREMER, and CNES through the international metaprogramme MISTRALS dedicated to the

understanding of the Mediterranean basin environmental processes (http://www.mistrals-home.org), by the ANR-12-BS06-0003 ASICS-MED, and by the EU-FP7 PERSEUS (GA 287600), JERICO (GA 262584), and GROOM (GA 284321). Five Argo floats were provided by LEFE/GMMC. Important data sets were provided by the MOOSE (ALLENVI-INSU) and MERMEX-DEWEX French programmes. Large amounts of data are available in the HyMeX database for non-commercial research. Others, such as Argo and glider profiles, are archived in the CORIOLIS data centre for operational oceanography.

References

Andreas, E.L., P.O.G. Persson, and J.E. Hare. 2008. A bulk turbulent air-sea flux algorithm for high-wind, spray conditions, *Journal of Physical Oceanography* 38, 1581-1596, doi: 10.1175/2007JPO3813.1.

Belamari, S., and A. Pirani. 2007. Validation of the optimal heat and momentum fluxes using the ORCA-LIM global ocean-ice model. *MERSEA IP Deliverable*, D.4.1.3, 88pp.

Bignami, F., S. Marullo, R. Santoleri, and M.E. Schinao. 1995. Longwave radiation budget in the Mediterranean Sea, *Journal of Geophysical Research* 100, C2, 2501-2514.

Bosse, A., P. Testor, L. Houpert, P. Damien, L. Prieur, D. Hayes, V. Taillandier, X. Durrieu de Madron, F. D'Ortenzio, L. Coppola, J. Karstensen, and L. Mortier. 2016. Scales and dynamics of Submesoscale Coherent Vortices formed by deep convection in the northwestern Mediterranean Sea, *Journal of Geophysical Research* 121, doi:10.1002/2016JC012144.

Bourras, D., A. Weill, G. Caniaux, L. Eymard, B. Bourlès, S. Letourneur, D. Legain, E. Key, F. Baudin, B. Piguet, O. Traullé, G. Bouhours, B. Sinardet, J. Barrié, J. P. Vinson, F. Boutet, C. Berthod and A. Clémençon. 2009. Turbulent air-sea fluxes in the Gulf of Guinea during the AMMA experiment. *Journal of Geophysical Research* 114, C04014, doi:10.1029/2008JC004951.

Callies, J., R. Ferrari, J.M. Klymak, and J. Gula. 2015. Seasonality in submesoscale turbulence. *Nature Communications* 6 :6862.

Canut, G., M. Lothon, F. Saïd, and F. Lohou. 2010. Observation of entrainment at the interface between monsoon flow and the Saharan Air Layer. *Quarterly Journal of the Royal Meteorological Society* 136, 34-46.

Doerenbecher, A., C. Basdevant, P. Drobinski, P. Durand, C. Fesquet, F. Bernard, P. Cocquerez, N. Verdier, and A. Vargas. 2016. Low atmosphere drifting balloons: platforms for environment monitoring and forecast improvement. *Bulletin of the American Meteorological Society* doi:10.1175/BAMS-D-14-00182.1

Drobinski, P., V. Ducrocq, P. Alpert, E. Anagnostou, K. Béranger, M. Borga, I. Braud, A. Chanzy, S. Davolio, G. Delrieu, C. Estournel, N. Filali Boubrahmi, J. Font, V. Grubisic, S. Gualdi, V. Homar, B. Ivancan-Picek, C. Kottmeier, V. Kotroni, K. Lagouvardos, P. Lionello, M.C. Llasat, W. Ludwig, C. Lutoff, A. Mariotti, E. Richard, R. Romero, R. Rotunno, O. Roussot, I. Ruin, S. Somot, I. Taupier-Letage, J. Tintore, R. Uijlenhoet, and H. Wernli. 2014. HyMeX, a 10-year multidisciplinary program on the Mediterranean water cycle. *Bulletin of the American Meteorological Society* 95, 1063-1082, doi: 10.1175/BAMS-D-12-00242.1

Ducrocq, V., I. Braud, S. Davolio, R. Ferretti, C. Flamant, A. Jansa, N. Kalthoff, E. Richard, I. Taupier-Letage, P.A. Ayral, S. Belamari, A. Berne, M. Borga, B. Boudevillain, O. Bock, J.L. Boichard, M.N. Bouin, O. Bousquet, C. Bouvier, J. Chiggiato, D. Cimini, U. Corsmeier, L. Coppola, P. Cocquerez, E. Defer, J. Delanoë, P. Di Girolamo, A. Doerenbecher, P. Drobinski, Y. Dufournet, N. Fourrié, J.J. Gourley, L. Labatut, D. Lambert, J. Le Coz, F.S. Marzano, G. Molinié, A. Montani, G. Nord, M. Nuret, K. Ramage, B. Rison, O. Roussot, F. Said, A. Schwarzenboeck, P. Testor, J. Van Baelen, B. Vincendon, M. Aran, and J. Tamayo. 2014. HyMeX-SOP1, the field campaign dedicated to heavy precipitation and flash-flooding in the Northwestern Mediterranean. *Bulletin of the American Meteorological Society* 95, 1083-1100, doi: 10.1175/BAMS-D-12-00244.1

Estournel, C, P. Testor, P. Damien, F. D'Ortenzio, P. Marsaleix, P. Conan, F. Kessouri, X. Durrieu de Madron, L. Coppola, J.M. Lellouche, S. Belamari, L. Mortier, C. Ulses, M.N. Bouin, and L. Prieur. 2016. High resolution modelling of dense water formation in the North-Western

Mediterranean during winter 2012–2013: processes and budget. *Journal of Geophysical Research* 121(7):5367–5392. doi:10.1002/2016JC011935

Fairall, C.W, E.F. Bradley, J.E. Hare, A.A. Grachev, and J.B. Edson. 2003. Bulk parameterization of air-sea fluxes: updates and verification for the COARE algorithm, *Journal of Climate* 16, 571-591.

Fourrié, N., E. Bresson, M. Nuret, C. Jany, P. Brousseau, A. Doerenbecher, M.Kreitz, O. Nuissier, E. Sevault, H. Bénichou, M. Amodei, and F. Pouponneau. 2015. AROME-WMED, a real-time mesoscale model designed for the HyMeX special observation periods. *Geoscientific Model Development* 8, 1919-1941, doi:10.5194/gmd-8-1919-2015.

Giordani, H., L. Prieur and G. Caniaux. 2006. Advanced insights into sources of vertical velocity in the ocean. *Ocean Dynamics* 56(5-6) :513–524

Hauser, D., H. Branger, S. Bouffies-Cloché, S. Despiau, W. Drennan, H. Dupuis, P. Durand, X. Durrieu de Madron, C. Estournel, L. Eymard, C. Flamant, H. Graber, C. Guérin, K. Kahma, G. Lachaud, J.M. Lefèvre, J. Pelon, H. Pettersson, B. Piguet, P. Queffeulou, D. Taillez, J. Tournadre, and A. Weill. 2003. The FETCH experiment : an overview. *Journal of Geophysical Research* 108, C3, pages 1-1 to 1-15. doi:10.1029/2001JC001202

Herrmann, M., S. Somot, F. Sevault, C. Estournel, and M. Déqué. 2008. Modeling the deep convection in the northwestern Mediterranean Sea using an eddy-permitting and an eddy-resolving model: Case study of winter 1986–1987, *Journal of Geophysical Research* 113, C04011, doi:10.1029/2006JC003991.

Houpert, L., X. Durrieu de Madron, P. Testor, A. Bosse, F. D'Ortenzio, M.N. Bouin, D. Dausse, H. Le Goff, S. Kunesch, M. Labaste, L. Coppola, L. Mortier, and P. Raimbault. 2016. Observations of open-ocean deep convection in the northwestern Mediterranean Sea: Seasonal and interannual variability of mixing and deep water masses for the 2007–2013 period. *Journal of Geophysical Research* doi:10.1002/2016JC011857

Marsaleix, P., F. Auclair, T. Duhaut, C. Estournel, C. Nguyen, and C. Ulses. 2012. Alternatives to the Robert-Asselin filter. *Ocean Modelling* 41, 53-66, doi:10.1016/j.ocemod.2011.11.002

Marshall, J., and F. Schott. 1999. Open-ocean convection: Observations, theory, and models. *Reviews of Geophysics* 37(1):1–64. doi: 10.1029/98RG02739.

MEDOC Group. 1970. Observations of formation of deep-water in the Mediterranean Sea, 1969. *Nature* 227, 1037–1040.

Mertens, C., and F. Schott. 1998. Interannual variability of deep-water formation in the northwestern Mediterranean. *Journal of Physical Oceanography* 28, 1410-1424.

Moon, I.J., I. Ginis, T. Hara, and B. Thomas. 2007. A physics-based parameterization of air-sea momentum flux at high wind speeds and its impact on hurricane ontensity predictions, *Monthly Weather Review* 135, 2869-2878, doi: 10.1175/MWR3432.1.

Oost, W.A., G.J. Komen, C.M.J. Jacobs, and C. Van Oort. 2002. New evidence for a relation between wind stress and wave age from measurements during ASGAMAGE, *Boundary-Layer Meteorology* 103, 409-438.

Send, U., J. Font, and C. Mertens. 1996. Recent observation indicates convection's role in deep water circulation. *Eos, Transactions American Geophysical Union* 77 (7), 61–65.

Somot, S., L. Houpert, F. Sevault, P.Testor, A. Bosse, I. Taupier-Letage, M.N. Bouin, R. Waldman, C. Cassou, E. Sanchez-Gomez, X. Durrieu de Madron, F. Adloff, P. Nabat and M. Herrmann. 2016. Characterizing, modelling and understanding the climate variability of the deep water formation in the North-Western Mediterranean Sea. *Climate Dnamics* doi:10.1007/s00382-016-3295-0

Taylor, P.K. and M.J. Yelland. 2001. The dependence of sea surface roughness on the height and steepness of the waves. *Journal of Physical Oceanography* 31, 572-590.

Testor, P., and J.C. Gascard. 2006. Post-convection spreading phase in the Northwestern Mediterranean Sea. *Deep-Sea Research Part I* 53, 869–893.

Thomas, L. N., J.R. Taylor, R. Ferrari, and T.M. Joyce. 2013. Symmetric instability in the Gulf Stream. *Deep-Sea Research Part II* 91, 96–110, doi:10.1016/j.dsr2.2013.02.025.

Visbeck, M., J. Marshall, and H. Jones. 1996. Dynamics of Isolated Convective Regions in the Ocean. *Journal of Physical Oceanography* 26, 1721-1734.

Waldman, R., S. Somot, M. Herrmann, P. Testor, C. Estournel, F. Sevault, L. Prieur, L. Mortier, L. Coppola, V. Taillandier, P. Conan, and D. Dausse. 2016. Estimating dense water volume and its

559 evolution for the year 2012-2013 in the North-western Mediterranean Sea: an Observing System
560 Simulation Experiment approach. *Journal of Geophysical Research* doi:10.1002/2016JC011694
561

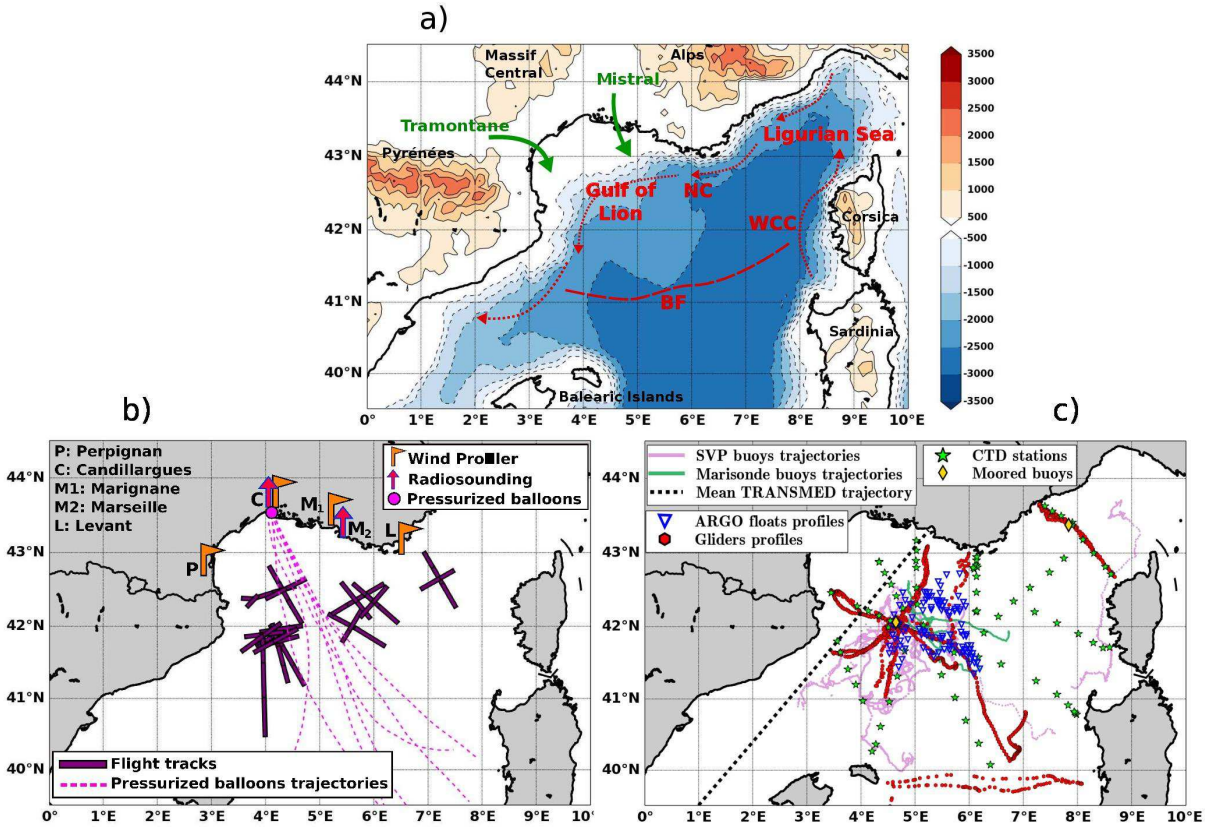

Figure 1: (a) Geographical characteristics of the north-western Mediterranean and main oceanic characteristics NC: Northern Current, BF: North Balearic Front, WCC: West Corsica Current and typical winds producing dense water formation; (b) Fixed instruments and typical trajectories of the balloons and aircraft documenting the atmospheric boundary layer; (c) Positions of the different platforms participating to the sounding of the ocean.

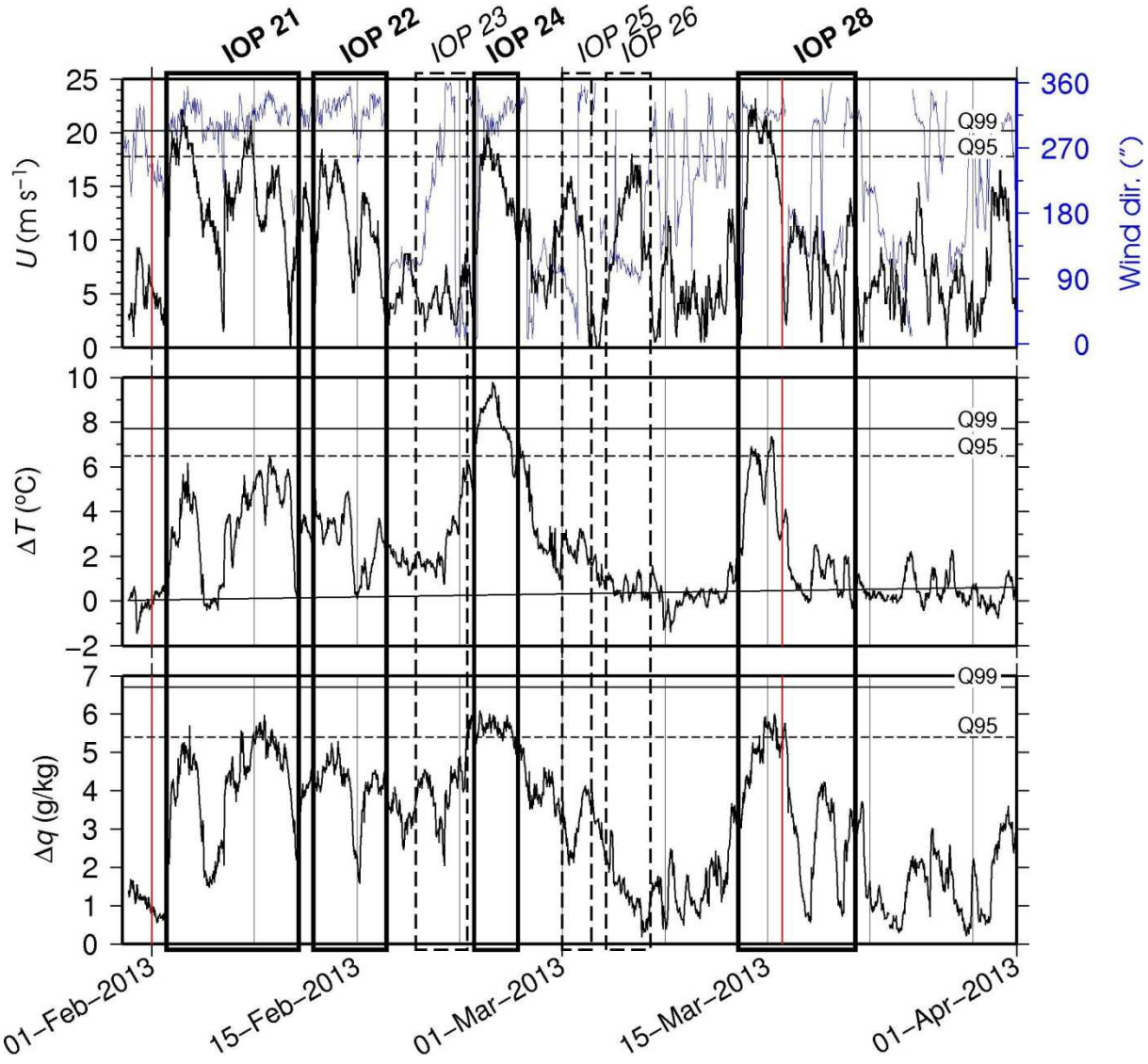

Figure 2: Time series of 10-m wind speed (top, black, m/s) and direction (top, blue, degrees from N), surface temperature gradient (middle, SST - 2-m air temperature, °C), and surface specific humidity gradient (bottom) observed at the LION buoy during the SOP2 time period. Intense Observation Periods (IOPs) are shown by solid frames for those corresponding to Mistral/Tramontane events, dashed frames for those corresponding to other conditions (see text). Solid (resp. dashed) horizontal lines indicate the Q99 (resp. Q95) limits with respect to the 2002-2011 climatology (see text).

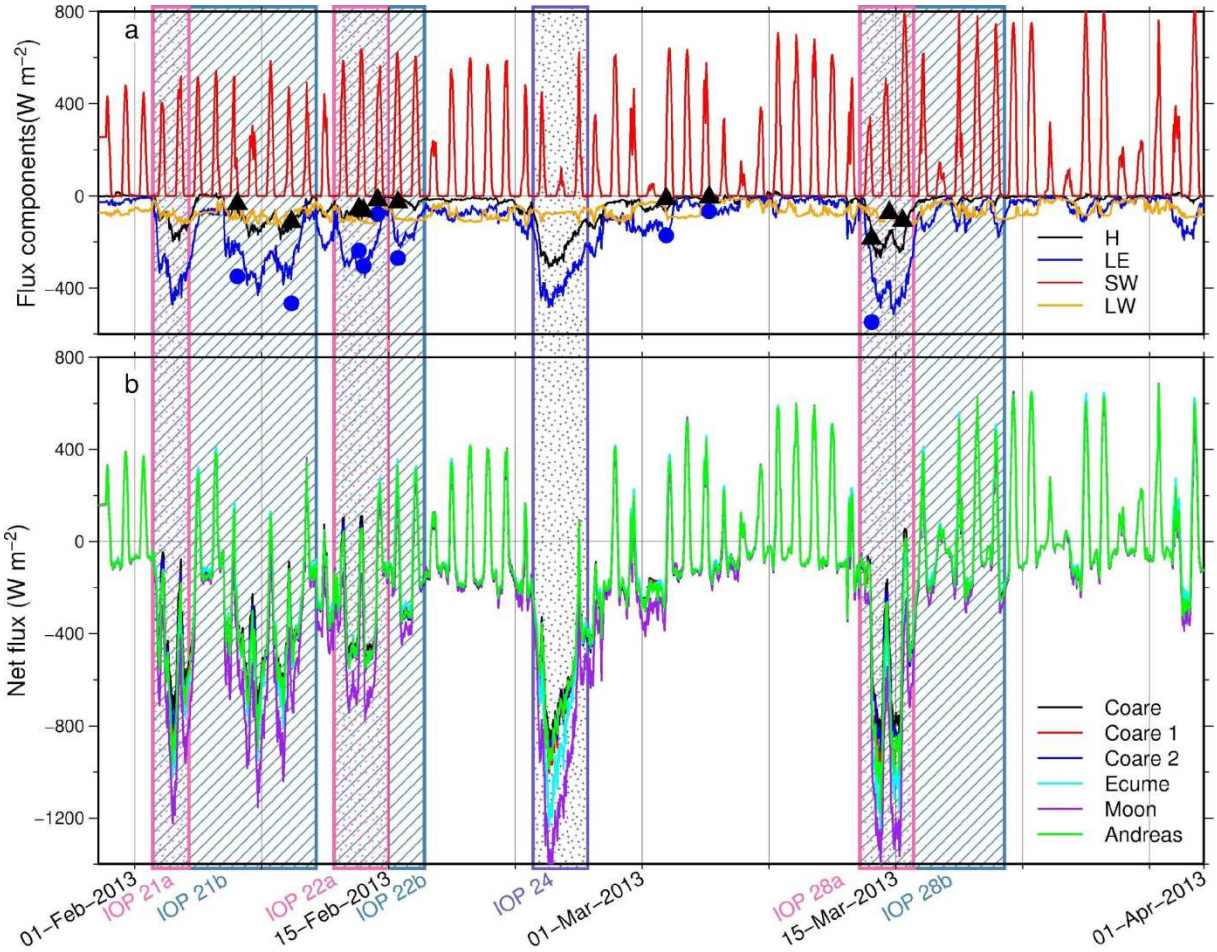

581

582 Figure 3 : a) Time series of the radiative and turbulent fluxes during the SOP2 time period (W/m^2).
583 Sensible heat flux (H, black), latent heat flux (LE, blue), short-wave radiative flux (SW, red) and long-
584 wave radiative flux (LW, orange) are computed from the Lion buoy observed parameters using the
585 COARE 3.0 (Fairall et al., 2003) algorithm for the turbulent part and the Bignami et al., 1995 formulae
586 for the upward radiative part. Blue circles and black triangles represent respectively the latent and
587 sensible heat fluxes measured by the aircraft along its lowest legs.
588 b) Time series of the net heat flux (W/m^2) on the same period, computed using different bulk
589 formulae. black : Coare, (Fairall et al., 2003) without wave impact; red: Coare 1 with wave-age effect;
590 blue : Coare 2 with peak period and significant height effects; cyan : Ecume, (Belamari and Pirani,
591 2007); purple : Moon, (Moon et al., 2007); green: Andreas, (Andreas et al., 2008). Intense
592 Observation Periods (IOP) corresponding to Mistral/Tramontane events are indicated in pink, to DWF
593 and Mistral/Tramontane events in purple, and to DWF only (no strong wind) in blue.

594

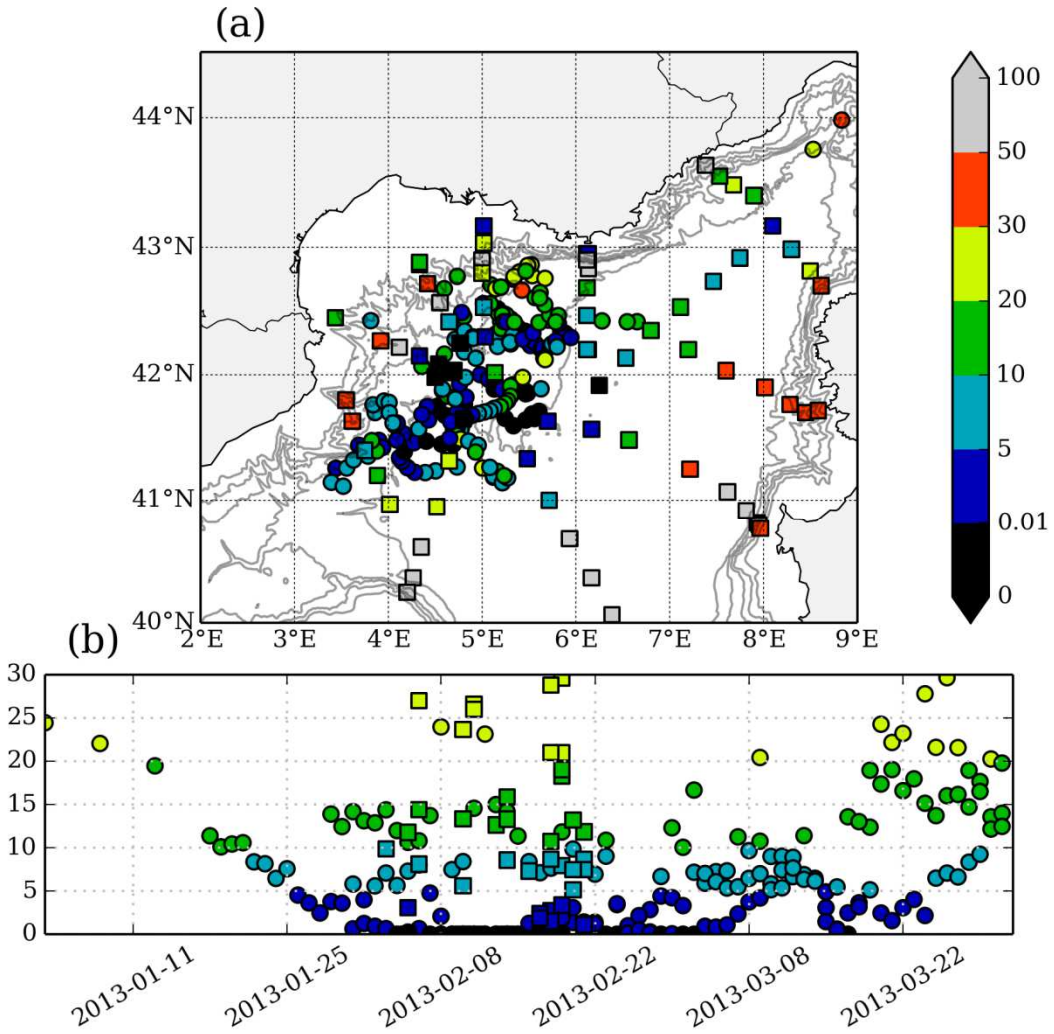

Figure 4: Spatial distribution (a) and time evolution from January 2012 to March 2013 (b) of the stratification index SI relative to 1500 m (kg m^{-2}) calculated from the CTD (square) and the Argo floats (circles). Note that only the stratification indices lower than 30 kg m^{-2} have been plotted in the bottom panel.

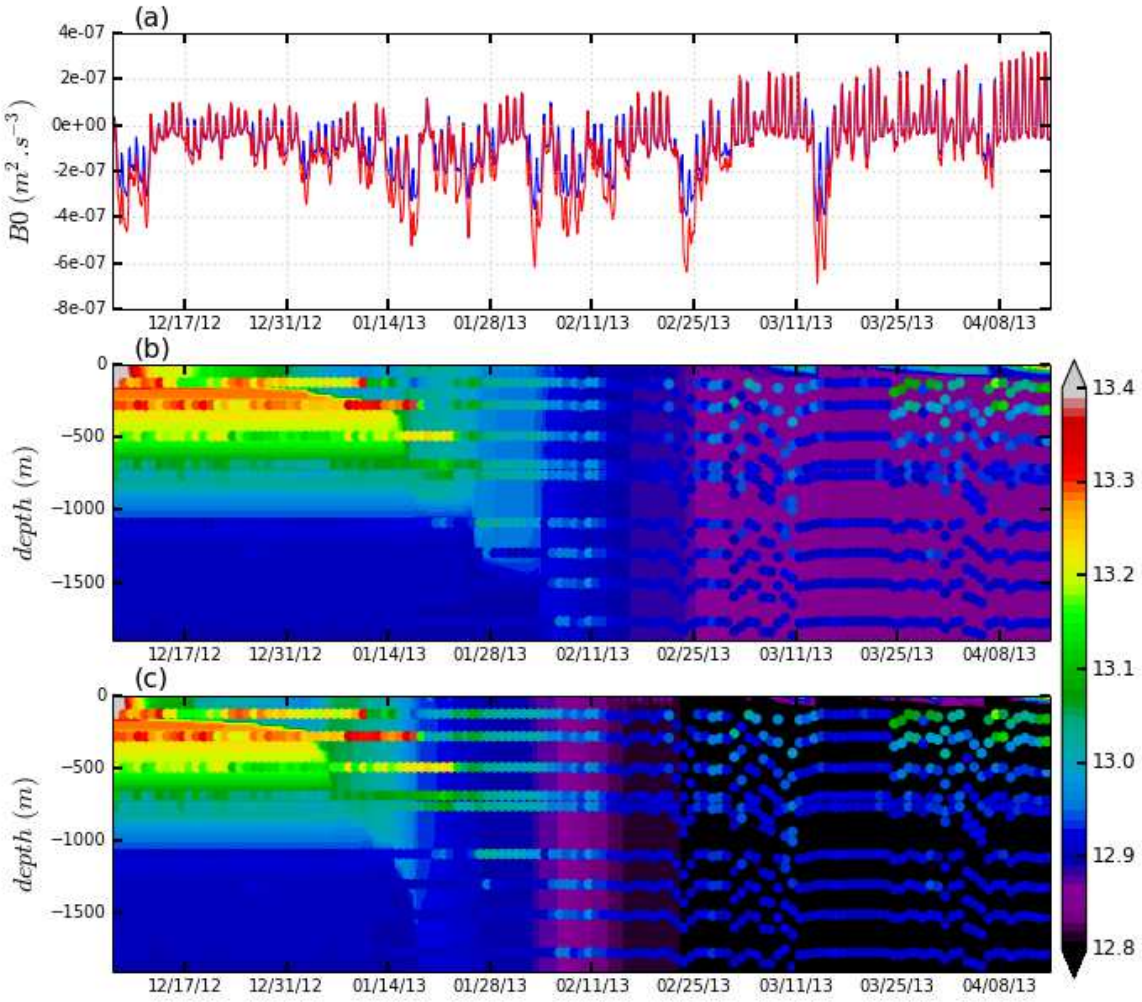

603 Figure 5: (a) Time series of the surface buoyancy flux (m^{-2} s^{-3}) for COARE (blue) and MOON (red)
604 simulations ; (b) and (c) Hov-Moller of temperature simulated at the LION mooring with a 1DV
605 model for COARE and MOON simulations respectively. Temperature measured at the LION mooring
606 is superimposed with open circles.

607

608

609

610

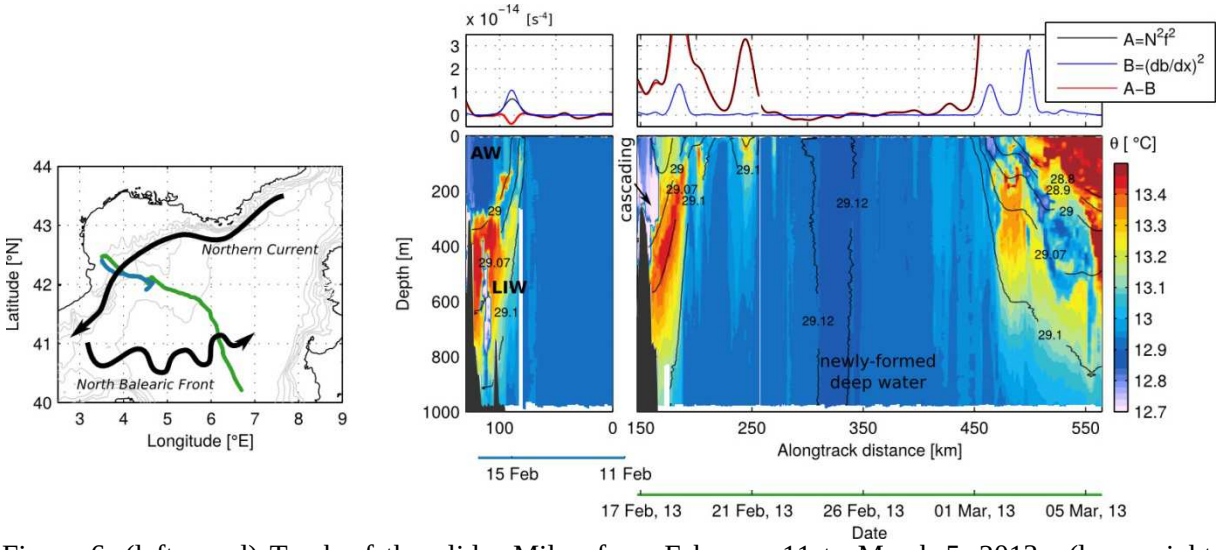

611

612 Figure 6: (left panel) Track of the glider Milou from February 11 to March 5, 2013. (lower right

613 panel): Potential temperature section with black lines showing isopycnals; (upper right panel):

614 Potential vorticity averaged between 50 m and 100 m (in red) decomposed into two terms: A (in blue)

615 associated with the lateral buoyancy gradients and B (in black) with the vertical stratification.

616

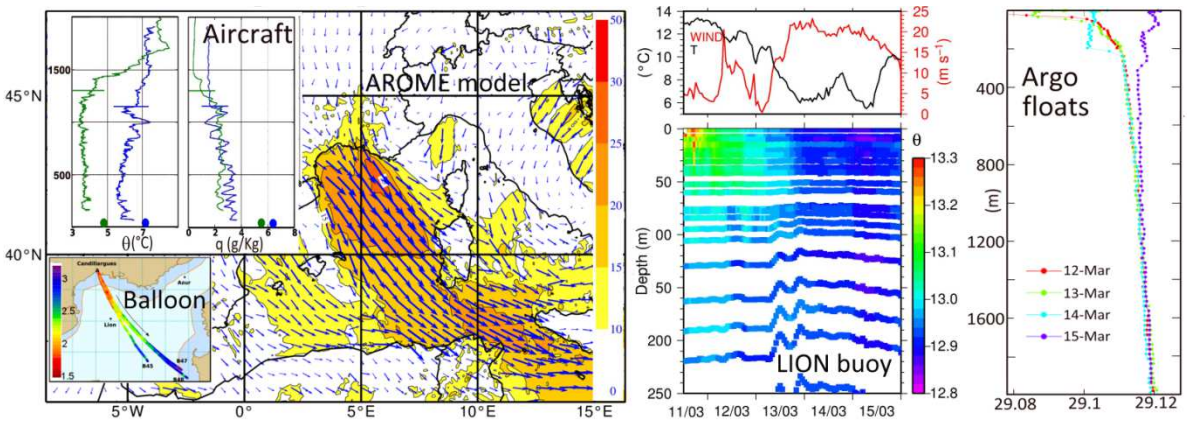

Figure 7: Illustrations of an intense observation period (IOP28).

Left panel (AROME model): background: wind at 10 m from AROME-WMED model on March 14 at 00 UTC, (Aircraft insert): profiles of wind speed, potential temperature and water vapour mixing ratio measured by the aircraft on 14 (blue lines) and 15 (green lines) March in the Gulf of Lion; the dashed lines mark the top of the ABL, the surface values measured at the LION buoy during the flights are indicated on the bottom of each diagram, (Balloon insert): air specific humidity (g/Kg) recorded by three balloons flying between 600 and 900 m on 14 and 15 March; rapid variations of humidity are the results of rapid vertical excursions of the balloons (*e.g.* at the end of flight 48), the orange polygon shows the authorized flight domain.

Middle panel (LION buoy): (top) air temperature in black and wind in red, (bottom) sea temperature under the buoy.

Right panel (Argo floats): potential density recorded by Argo float 6901471 between 12 and 15 March. The low values of surface density (~29.04) on March 12 are not shown for the clarity of the figure.